Geology, published online on 10 January 2014 as doi:10.1130/G35001.1

Seismic evidence for a crustal magma reservoir beneath the upper east rift zone of Kilauea volcano, Hawaii

Guoqing Lin[1], Falk Amelung[1], Yan Lavallée[2], and Paul G. Okubo[3]
[1]Division of Marine Geology and Geophysics, Rosenstiel School of Marine and Atmospheric Science, University of Miami, Miami, Florida 33149, USA
[2]Geology and Geophysics, University of Liverpool, Liverpool L69 3GP, UK
[3]Hawaiian Volcano Observatory, U.S. Geological Survey, Hawaii Volcanoes National Park, Hawaii 96718, USA

ABSTRACT

An anomalous body with low Vp (compressional wave velocity), low Vs (shear wave velocity), and high Vp/Vs anomalies is observed at 8–11 km depth beneath the upper east rift zone of Kilauea volcano in Hawaii by simultaneous inversion of seismic velocity structure and earthquake locations. We interpret this body to be a crustal magma reservoir beneath the volcanic pile, similar to those widely recognized beneath mid-ocean ridge volcanoes. Combined seismic velocity and petrophysical models suggest the presence of 10% melt in a cumulate magma mush. This reservoir could have supplied the magma that intruded into the deep section of the east rift zone and caused its rapid expansion following the 1975 M7.2 Kalapana earthquake.

INTRODUCTION

Kilauea volcano in Hawaii is currently the most active volcano in the world, producing more than 1.2 km^3 of lava every 10 yr (Poland et al., 2012). Although the structure of the volcano has been extensively studied, only the shallow part of the magma plumbing system has been resolved in part. Magma ascends vertically through a primary conduit to a reservoir at 2 km depth beneath the summit caldera, i.e., 1 km below sea level (bsl) (Ryan, 1987; Dawson et al., 1999). From there it is thought to travel through open conduits and erupt at Pu‘u‘O‘o crater as well as in a lava lake within Halema‘uma‘u crater, where it degasses, loses its buoyancy, and collapses. Another magma storage zone that is thought to take the form of a stacked sill plexus (Baker and Amelung, 2012) is located south of the caldera at 2–3 km bsl. Geochemical studies support the presence of one or more shallow magma reservoirs in the summit area (Pietruszka and Garcia, 1999), and pockets of highly differentiated magma stored within the rift zones (Helz and Wright, 1992). Three-dimensional (3-D) seismic tomography also shows evidence of shallow magma sources beneath Kilauea (Thurber, 1984; Dawson et al., 1999).

Little is known about the deeper part of the magma plumbing system (within the lower volcanic pile, the oceanic crust, and the uppermost mantle). Petrologic data provide evidence for magma in the deep rift zone (Wright and Helz, 1996). Geodetic studies infer a deep inflating dike in the lower part of the volcanic pile beneath the east rift zone to explain the seaward motion of the south flank (Cayol et al., 2000; Owen et al., 2000). The presence of a large magma storage area was suggested in the lower part of the volcanic pile based on the lack of earthquake hypocentral locations (Ryan, 1988; Denlinger, 1997). Seismic velocity studies showed high compressional wave velocities (Vp) beneath the summit and rift zones extending to a depth of 9 km; the data were interpreted as indicating a volcanic core composed of ultramafic cumulates that settled from the active magma system above (e.g., Okubo et al., 1997; Park et al., 2007, 2009). Previously observed low Vp/Vs (the ratio of compressional to shear wave velocity) ratios are inconsistent with the existence of a sizable molten body at depth beneath the east rift zone (Hansen et al., 2004).

Here we present a new three-dimensional (3-D) seismic velocity model from simultaneous inversions of variations in Vp, Vp/Vs, and earthquake locations. We observe an anomalous body with low Vp, low Vs, and high Vp/Vs values in the oceanic crust below Mauna Ulu vent in the upper east rift zone, which we interpret as a crustal magma reservoir. This reservoir could have supplied the magma that intruded into the deep section of the east rift zone following the 1975 M7.2 Kalapana earthquake, associated with rapid expansion of the rift zone.

DATA AND METHODS

The seismic data used for the tomographic inversions are the first-arrival times of the compressional and shear waves from ~53,000 events on and near the Island of Hawaii between A.D. 1992 and 2009, recorded by the seismic stations of the Hawaiian Volcano Observatory (HVO) (Fig. 1A). Most of these events are >M1.0, consisting of 1.4×10^6 first arrivals picked by HVO analysts. Approximately 80,000 more events with only waveform data (i.e., no phase picks are available) were used for the relative location improvements by Matoza et al. (2013), but were not used in this study. We selected 1817 composite events with 64,863 P wave and 25,438 S wave picks for the inversion by using the master event selection method presented by Lin et al. (2007b).

We apply the SIMUL2000 tomographic algorithm (Thurber and Eberhart-Phillips, 1999) to invert for Vp, Vp/Vs variations, and earthquake locations using P wave and S-P arrival times simultaneously. The final Vs model is obtained by dividing the Vp by the Vp/Vs model. Our model is represented by nodes in a uniform 3 km grid in the horizontal dimension. The vertical nodes are positioned at −1, 1, 3, 6, 9, 12, 15, 20, 25, and 35 km depth (relative to mean sea level; note that depths herein are relative to mean sea level). We start with a 1-D velocity model (Klein, 1981). The constant starting Vp/Vs ratio of 1.74 for the inversion gives the optimal fit among different tested values between 1.68 and 1.79. Damping parameters are selected using a data misfit versus model variance tradeoff analysis. After we obtain the final velocity model, we relocate all the events with phase picks using the resulting 3-D velocity model, similar-event cluster analysis, and differential-time relocation methods similar to those in Lin et al. (2007a).

RESULTS

Figure 1B shows map views of the final Vp, Vs, and Vp/Vs perturbations relative to the 1-D starting models at three depth slices. Zero depth in our model corresponds to mean sea level. At 6 km depth, we observe high Vp anomalies (blue in Fig. 1B, panel A) near the caldera, the upper-middle east rift zone, and part of the southwest rift zone, and low Vp anomalies (red) near the Hilina fault system and the lower east rift zone. The Vs model shows largely high-velocity anomalies (Fig. 1B, panel B). High Vp/Vs ratios occur near the caldera and in the southwest rift zone (blue), and low ratios are near the east rift and the Koae fault zone (red in Fig. 1B, panel C). The high Vp and low Vp/Vs in the east rift zone can be best explained by a combination of mafic compositions rather than single composition models, as indicated by the petrologic model of Shillington et al. (2013) for another tectonic setting. At 9 km depth, the velocity contrasts become weaker (Fig. 1B, panels D–F). High Vp anomalies occur near the caldera and the southwest and middle east rift zones and low Vp anomalies occur in the south flank, the upper and lower east rift zones, and near the Hilina fault zone (Fig. 1B, panel D). High Vs anomalies occur under the caldera and the Hilina fault system and low Vs anomalies occur north of the Koae fault system and under the southwest rift zone (Fig. 1B, panel D). The

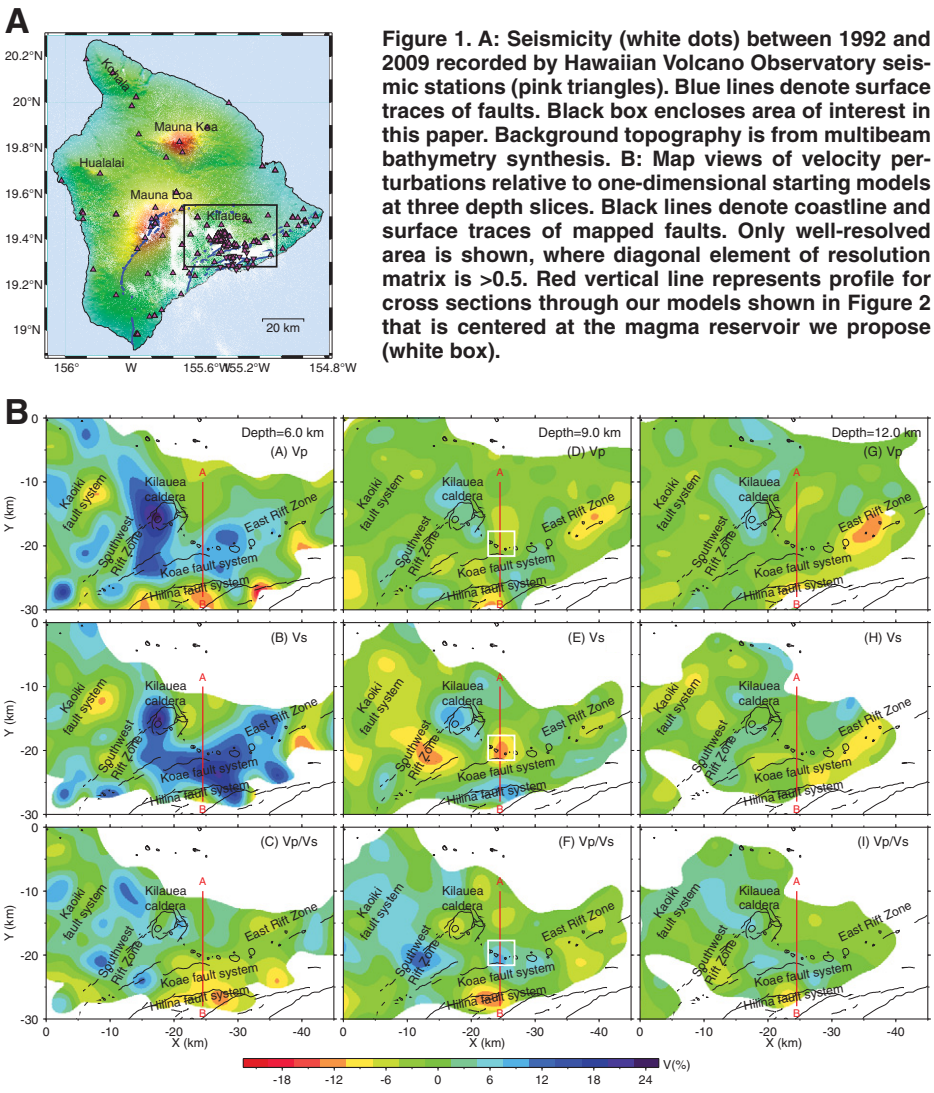

Figure 1. A: Seismicity (white dots) between 1992 and 2009 recorded by Hawaiian Volcano Observatory seismic stations (pink triangles). Blue lines denote surface traces of faults. Black box encloses area of interest in this paper. Background topography is from multibeam bathymetry synthesis. B: Map views of velocity perturbations relative to one-dimensional starting models at three depth slices. Black lines denote coastline and surface traces of mapped faults. Only well-resolved area is shown, where diagonal element of resolution matrix is >0.5. Red vertical line represents profile for cross sections through our models shown in Figure 2 that is centered at the magma reservoir we propose (white box).

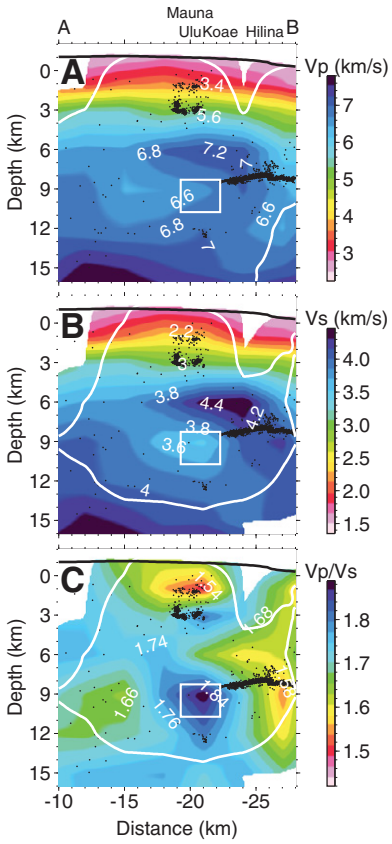

Figure 2. Cross sections through the resulting Vp, Vs (compressional and shear wave velocities), and Vp/Vs models along profile A-B shown in Figure 1. Black dots represent relocated background seismicity by using waveform cross-correlation data within ±3 km distance of the profile line. White contours enclose regions with resolution >0.5. White box marks area where our proposed magma reservoir is located.

Vp/Vs model (Fig. 1B, panel F) shows high ratios (perturbations of 10%–15%) in the areas of low Vs anomalies, and low ratios (perturbations of −10%) under the Hilina fault system. At 12 km depth, similar velocity patterns are observed, with a high Vp anomaly under the caldera and a low Vp anomaly under the east rift zone (Fig. 1B, panel G). The Vs model shows correlations with the Vp model, except that the well-resolved area is smaller (Fig. 1B, panel H). The Vp/Vs perturbations at this depth are <7% (Fig. 1B, panel I).

We propose that a magma reservoir coincides with the isolated low-Vp, low-Vs, and high-Vp/Vs anomaly at 9 km depth beneath Mauna Ulu in the upper east rift zone (white box in Fig. 1B, panels D–F). The north-south cross sections through the models show that this body is located within an aseismic zone at depths of 8–11 km (Fig. 2). The velocity within this body and the layer-average values at different depths are summarized in Table 1.

The seismic velocity inversion reveals another high Vp/Vs anomaly located at the same depth interval under the southwest rift zone (Fig. 1B, panel F). We do not interpret this anomaly as a magma body because it is not associated with a consistently low Vp anomaly (see Fig. DR1 in the GSA Data Repository[1]). Another significant feature seen in the cross sections is a zone of high Vp, high Vs, and low Vp/Vs under the Koae fault system at 5–8 km depth, which Okubo et al. (1997) interpreted as cumulates of the volcanic core.

The precise earthquake relocations based on the new 3-D velocity model provide constraints for the current debate as to whether Kilauea's slow slip events (Brooks et al., 2006) occur along the décollement or along zones of weakness at a shallower depth (Segall et al., 2006; Wolfe et al., 2007). Our study places most of the lower south flank seismicity along a linear subhorizontal structure at 8–8.5 km depth (Fig. 2), including triggered seismicity on the same fault inward from the slow slip events (Segall et al., 2006). This supports the inference by Syracuse et al. (2010) that the slow slip events occur along the décollement at this depth. Note that we only relocate earthquakes with phase picks available (40% of the entire event catalog) in order to improve absolute locations by using the new 3-D velocity model.

MELT FRACTION

To understand the nature of the east rift zone velocity anomaly, we investigate the variation of seismic velocities in partially molten rocks with melt fraction. We assume that this anomaly corresponds to a magma body comprised of olivine with fractional interstitial melt. This reservoir is subjected to lithostatic pressure approximated at 250 MPa, based on a density nearing 3.20 g/cm^3. A reservoir temperature of 1200 K was estimated by iterating the most appropriate pressure-temperature-melt fraction conditions through the

[1]GSA Data Repository item 2014066, supplemental information (Figures DR1–DR8) for the southwest rift zone anomaly and model resolution, is available online at www.geosociety.org/pubs/ft2014.htm, or on request from editing@geosociety.org or Documents Secretary, GSA, P.O. Box 9140, Boulder, CO 80301, USA.

TABLE 1. SEISMIC VELOCITIES FROM TOMOGRAPHIC INVERSION AND PARTIAL MELT PORTION BELOW THE UPPER EAST RIFT ZONE, KILAUEA

Depth (km)	Vp (km/s)	Vs (km/s)	Vp/Vs	Partial melt (%)
6	6.69	3.84	1.74	-
9	6.82	3.92	1.74	-
12	7.00	4.02	1.74	-
Anomalous body (9 km)	6.60	3.55	1.86	~10
High-velocity body (above)	7.20	4.40	1.64	-

Note: Compressional and shear wave velocities (Vp, Vs) at 6, 9, and 12 km depths are layer-average values for the area shown in Figure 2. The densities of the solid rocks range from 2.95 to 2.99 g/cm^3. Dash indicates "not applicable."

thermodynamic calculator MELTS (Asimow and Ghiorso, 1998), cross-referenced against our combined seismic velocity–petrological model. The latter was constructed as there are no laboratory measurements of the seismic velocities of partially molten dunite at the temperature and pressure conditions of our proposed magma reservoir. To estimate the effect of melt on Vp and Vs of a partially molten rock, we use the measurements for a synthetic crystal-liquid suspension of Caricchi et al. (2008), who determined that each percent of interstitial melt leads to a decrease in Vp and Vs of ~1.43% and 1.49%, respectively. This relationship is consistent with velocity models for partially molten rocks at mid-ocean ridges (e.g., Mainprice, 1997). Of importance for our purposes, Vp and Vs are only weakly dependent on iron content, and therefore Fe-Mg differentiation between the liquid and crystalline phases should not affect the melt estimate for olivine cumulates (Liu et al., 2005). Seismic velocities are also weakly dependent on pressure (P) and temperature (T) within the ranges of interest [dVp/dP is ~0.2 km/s/GPa (Aizawa et al., 2001), dVp/dT is –0.51 m/s/K, and dVs/dT is –0.39 m/s/K (Isaak, 1992)]. At 10 km depth (250 MPa), Vp is reduced by 50 m/s, and at 1300 K, Vp and Vs are reduced by ~51 and 39 m/s with little dependence on the melt estimate.

We use the laboratory-measured velocities of olivine at 1200 K but ambient pressure (Vp = 7.955 km/s, Vs = 4.536 km/s, Vp/Vs = 1.754; Isaak, 1992) to infer the presence of ~10% melt from our estimated velocities of the anomalous body (Vp = 6.6 km/s, Vs = 3.55 km/s, Vp/Vs = 1.86). The inferred melt fraction is generally consistent with petrologic constraints (4%–9% melting) estimated from olivine-hosted melt inclusions in Kilauea (Norman et al., 2002). The Vp of the anomalous body is similar to that of the mush zone beneath the axial melt lens at fast-spreading mid-ocean ridges, which is characterized by a Vp decrease of 0.2–0.4 km/s relative to the surrounding crust (Sinha et al., 1998).

The observed anomalous body is a robust feature based on the synthetic data tests (Figs. DR2–DR8 in the Data Repository). Its presence shows no strong dependence on the location of the inversion nodes. However, our tomography model is relatively smooth and the small-scale (1–2 km) velocity structure may not be resolved given the data and station distributions in this study. Due to the use of damping parameters in the inversion, the melt fraction should be considered as a lower bound (i.e., the inversion tends to underestimate the absolute velocity anomalies.)

DISCUSSION AND INTERPRETATION

The depth of the proposed magma body implies that it is located at the volcanic shield–oceanic crust interface, with the largest part embedded in the crust. A streak of seismicity is located south of and right above this body, which marks the horizontal décollement fault along the paleoseafloor on which the volcanoes grew. Although previous velocity studies suggested that melt might be within the oceanic crust (e.g., Hill and Zucca, 1987; Park et al., 2007), this is the first geophysical observation for magma storage under a Hawaiian volcano in its shield-building phase with a high rate of magma supply. It is consistent with the petrologically inferred crustal reservoir of Loihi, a submarine volcano also in its shield-building phase (Clague and Dixon, 2000). Magma reservoirs in the oceanic crust stand in contrast to deep magma reservoirs at the crust-mantle boundary (15–20 km depth) that are associated with late phases of Hawaiian volcanism (Frey et al., 1990; Clague and Dixon, 2000), when magma supply rates are too low to maintain shallow reservoirs.

Why would this magma pond beneath the volcanic pile? A picritic mush of fractionated olivine and 10% melt has a density of 3.1–3.2 g/cm^3 (for a melt density of 2.65 g/cm^3 and olivine density of 3.3 g/cm^3, a magma with 90% crystal content has a density of 3.2 g/cm^3). Although the density is inevitably lower because of dissolved volatiles (H_2O and CO_2) and exsolved CO_2 bubbles, it is still higher than the Vp-derived density of the surrounding oceanic crust (2.97 g/cm^3; density determined using the relation for basalt, diabase, and gabbro of Godfrey et al., 1997). Thus, the mush as a whole is not buoyant. Nevertheless, the melt may separate from the crystals, which cannot be detected by our model. Its relatively low density (2.65–2.70 g/cm^3) and, importantly, its very low viscosity enable its ascent.

However, the Hawaiian volcanoes are built on 60-m.y.-old oceanic crust and an ~200-m-thick layer of pelagic plus volcaniclastic sediments (Winterer, 1989), which act as a décollement along which the volcano spreads laterally in conjunction with large earthquakes (e.g., the A.D. 1868 M7.9 Pahala earthquake or the 1975 M7.2 Kalapana earthquake), aseismic creep (Owen et al., 2000), and slow slip events (Segall et al., 2006; Montgomery-Brown et al., 2010). The top of the magma body locates at the depth of these sediments, suggesting that they are a barrier for magma ascent. These sediments, possibly mechanically weakened by repeated seismic or aseismic slip, could have acted as a stress trap, deflecting vertical dikes to horizontal sills, which eventually grew into a reservoir (Gudmundsson, 2011). The anomalous body of interest could also be a remnant magma chamber that has persisted since the volcano was small.

The horizontal location of the magma body suggests that it may tap the deep magma supply route between the presumed melting site south of the island (Wright and Klein, 2006) and the primary conduit under the caldera. This has implications on how the volcano works. For example, it could have contributed the magma that intruded into the deep rift zone following the 1975 Kalapana earthquake. Magma movement in this part of the volcano is consistent with the repeated seismic activity at 5–7 km depth beneath Mauna Ulu reported for the years following the earthquake (Klein et al., 1987).

Crustal magma bodies are well documented for mid-ocean ridge volcanoes (Sinton and Detrick, 1992). A magma body reported for Fernandina volcano, Galapagos Islands, near the bottom of the volcanic pile, could be located within the oceanic crust (Bagnardi and Amelung, 2012). Our study suggests that deep crustal magma bodies could be much more widespread beneath oceanic island volcanoes than previously thought.

ACKNOWLEDGMENTS

We thank the U.S. Geological Survey Hawaiian Volcano Observatory for maintaining the seismic network and making the data available. We are grateful for the constructive and detailed comments by Julia Morgan, Michael Barton, and David Hill. Funding for this research was provided by National Science Foundation grant EAR-1246935. Lavallée acknowledges a SLiM (Strain Localisation in Magmas no. 306488) Starting Grant from the European Research Council.

REFERENCES CITED

Aizawa, Y., Ito, K., and Tatsumi, Y., 2001, Experimental determination of compressional wave velocities of olivine aggregate up to 1000 °C at 1 GPa: Tectonophysics, v. 339, p. 473–478, doi:10.1016/S0040-1951(01)00133-0.

Asimow, P., and Ghiorso, M., 1998, Algorithmic modifications extending MELTS to calculate subsolidus phase relations: American Mineralogist, v. 83, p. 1127–1132.

Bagnardi, M., and Amelung, F., 2012, Space-geodetic evidence for multiple magma reservoirs and subvolcanic lateral intrusions at Fernandina Volcano, Galapagos Islands: Journal of Geophysical Research, v. 117, B10406, doi:10.1029/2012JB009465.

Baker, S., and Amelung, F., 2012, Top-down inflation and deflation at the summit of Kilauea Volcano, Hawaii observed with InSAR: Journal of Geophysical Research, v. 117, B12406, doi:10.1029/2011JB009123.

Brooks, B.A., Foster, J.H., Bevis, M., Frazer, L.N., Wolfe, C.J., and Behn, M., 2006, Periodic slow earthquakes on the flank of Kilauea volcano, Hawaii: Earth and Planetary Science Letters, v. 246, p. 207–216, doi:10.1016/j.epsl.2006.03.035.

Caricchi, L., Burlini, L., and Ulmer, P., 2008, Propagation of P and S-waves in magmas with different crystal contents: Insights into the crystallinity of magmatic reservoirs: Journal of Volcanology and Geothermal Research, v. 178, p. 740–750, doi:10.1016/j.jvolgeores.2008.09.006.

Cayol, V., Dieterich, J., Okamura, A., and Miklius, A., 2000, High magma storage rates before the 1983 eruption of Kilauea, Hawaii: Science, v. 288, p. 2343–2346, doi:10.1126/science.288.5475.2343.

Clague, D.A., and Dixon, J.E., 2000, Extrinsic controls on the evolution of Hawaiian ocean island volcanoes: Geochemistry Geophysics Geosystems, v. 1, 1010, doi:10.1029/1999GC000023.

Dawson, P.B., Chouet, B.A., Okubo, P.G., Villasenor, A., and Benz, H.M., 1999, Three-dimensional velocity structure of the Kilauea caldera, Hawaii: Geophysical Research Letters, v. 26, p. 2805–2808, doi:10.1029/1999GL005379.

Denlinger, R.P., 1997, A dynamic balance between magma supply and eruption rate at Kilauea volcano, Hawaii: Journal of Geophysical Research, v. 102, p. 18091–18100, doi:10.1029/97JB01071.

Frey, F.A., Wise, W.S., Garcia, M.O., West, H., Kwon, S.T., and Kennedy, A., 1990, Evolution of Mauna Kea Volcano, Hawaii: Petrologic and geochemical constraints on postshield volcanism: Journal of Geophysical Research, v. 95, p. 1271–1300, doi:10.1029/JB095iB02p01271.

Godfrey, N.J., Beaudoin, B.C., and Klemperer, S.L., 1997, Ophiolitic basement to the Great Valley forearc basin, California, from seismic and gravity data: Implications for crustal growth at the North American continental margin: Geological Society of America Bulletin, v. 109, p. 1536–1562, doi:10.1130/0016-7606(1997)109<1536:OBTTGV>2.3.CO;2.

Gudmundsson, A., 2011, Deflection of dykes into sills at discontinuities and magma-chamber formation: Tectonophysics, v. 500, p. 50–64, doi:10.1016/j.tecto.2009.10.015.

Hansen, S., Thurber, C., Mandernach, M., Haslinger, F., and Doran, C., 2004, Seismic velocity and attenuation structure of the east rift zone and south flank of Kilauea volcano, Hawaii: Seismological Society of America Bulletin, v. 94, p. 1430–1440, doi:10.1785/012003154.

Helz, R.T., and Wright, T.L., 1992, Differentiation and magma mixing on Kilauea's east rift zone: Bulletin of Volcanology, v. 54, p. 361–384, doi:10.1007/BF00312319.

Hill, D.P., and Zucca, J.J., 1987, Geophysical constraints on the structure of Kilauea and Mauna Loa volcanoes and some implications for seismomagmatic processes, *in* Decker, R.W., et al., eds., Volcanism in Hawaii: Papers to commemorate the 75th anniversary of the founding of the Hawaiian Volcano Observatory: U.S. Geological Survey Professional Paper 1350, p. 903–917.

Isaak, D.G., 1992, High-temperature elasticity of iron-bearing olivines: Journal of Geophysical Research, v. 97, p. 1871–1885, doi:10.1029/91JB02675.

Klein, F.W., 1981, A linear gradient crustal model for south Hawaii: Seismological Society of America Bulletin, v. 71, p. 1503–1510.

Klein, F.W., Koyanagi, R.Y., Nakata, J.S., and Taxtigawa, W.R., 1987, The seismicity of Kilauea's magma system, *in* Decker, R.W., et al., eds., Volcanism in Hawaii: Papers to commemorate the 75th anniversary of the founding of the Hawaiian Volcano Observatory: U.S. Geological Survey Professional Paper 1350, p. 1019–1186.

Lin, G., Shearer, P.M., and Hauksson, E., 2007a, Applying a three-dimensional velocity model, waveform cross correlation, and cluster analysis to locate southern California seismicity from 1981 to 2005: Journal of Geophysical Research, v. 112, no. B12, doi:10.1029/2007JB004986.

Lin, G., Shearer, P.M., Hauksson, E., and Thurber, C.H., 2007b, A three-dimensional crustal seismic velocity model for southern California from a composite event method: Journal of Geophysical Research, v. 112, no. B11, doi:10.1029/2007JB004977.

Liu, W., Kung, J., and Li, B., 2005, Elasticity of San Carlos olivine to 8 GPa and 1073 K: Geophysical Research Letters, v. 32, L16301, doi:10.1029/2005GL023453.

Mainprice, D., 1997, Modelling the anisotropic seismic properties of partially molten rocks found at mid-ocean ridges: Tectonophysics, v. 279, p. 161–179, doi:10.1016/S0040-1951(97)00122-4.

Matoza, R., Shearer, P.M., Lin, G., Wolfe, C., and Okubo, P., 2013, Systematic relocation of seismicity on Hawaii Island from 1992 to 2009 using waveform cross-correlation and cluster analysis: Journal of Geophysical Research, v. 118, p. 2275–2288, doi:10.1002/jgrb.50,189.

Montgomery-Brown, E.K., Sinnett, D.K., Poland, M., Segall, P., Orr, T., Zebker, H., and Miklius, A., 2010, Geodetic evidence for en echelon dike emplacement and concurrent slow slip during the June 2007 intrusion and eruption at Kilauea volcano, Hawaii: Journal of Geophysical Research, v. 115, B07405, doi:10.1029/2009JB006658.

Norman, M., Garcia, M., Kamenetsky, V., and Nielsen, R., 2002, Olivine-hosted melt inclusions in Hawaiian picrites: Equilibration, melting, and plume source characteristics: Chemical Geology, v. 183, p. 143–168, doi:10.1016/S0009-2541(01)00376-X.

Okubo, P.G., Benz, H.M., and Chouet, B.A., 1997, Imaging the crustal magma sources beneath Mauna Loa and Kilauea volcanoes, Hawaii: Geology, v. 25, p. 867–870, doi:10.1130/0091-7613(1997)025<0867:ITCMSB>2.3.CO;2.

Owen, S., Segall, P., Lisowski, M., Miklius, A., Denlinger, R., and Sako, M., 2000, Rapid deformation of Kilauea Volcano: Global positioning system measurements between 1990 and 1996: Journal of Geophysical Research, v. 105, p. 18983–18998, doi:10.1029/2000JB900109.

Park, J., Morgan, J.K., Zelt, C.A., Okubo, P.G., Peters, L., and Benesh, N., 2007, Comparative velocity structure of active Hawaiian volcanoes from 3-D onshore-offshore seismic tomography: Earth and Planetary Science Letters, v. 259, p. 500–516, doi:10.1016/j.epsl.2007.05.008.

Park, J., Morgan, J.K., Zelt, C.A., and Okubo, P.G., 2009, Volcano-tectonic implications of 3-D velocity structures derived from joint active and passive source tomography of the island of Hawaii: Journal of Geophysical Research, v. 114, B09301, doi:10.1029/2008JB005929.

Pietruszka, A., and Garcia, M., 1999, A rapid fluctuation in the mantle source and melting history of Kilauea Volcano inferred from the geochemistry of its historical summit lavas (1790–1982): Journal of Petrology, v. 40, p. 1321–1342, doi:10.1093/petroj/40.8.1321.

Poland, M.P., Miklius, A., Sutton, A.J., and Thornber, C.R., 2012, A mantle-driven surge in magma supply to Kilauea Volcano during 2003–2007: Nature Geoscience, v. 5, p. 295–300, doi:10.1038/ngeo1426.

Ryan, M.P., 1987, Elasticity and contractancy of Hawaiian olivine tholeiite and its role in the stability and structural evolution of subcaldera magma reservoirs and rift systems, *in* Decker, R.W., et al., eds., Volcanism in Hawaii: Papers to commemorate the 75th anniversary of the founding of the Hawaiian Volcano Observatory: U.S. Geological Survey Professional Paper 1350, p. 1395–1447.

Ryan, M.P., 1988, The mechanics and three-dimensional internal structure of active magmatic systems—Kilauea volcano: Hawaii: Journal of Geophysical Research, v. 93, p. 4213–4248, doi:10.1029/JB093iB05p04213.

Segall, P., Desmarais, E., Shelly, D., Miklius, A., and Cervelli, P., 2006, Earthquakes triggered by silent slip events on Kilauea volcano, Hawaii: Nature, v. 442, p. 71–74, doi:10.1038/nature04938.

Shillington, D.J., Van Avendonk, H.J.A., Behn, M.D., Kelemen, P.B., and Jagoutz, O., 2013, Constraints on the composition of the Aleutian arc lower crust from Vp/Vs: Geophysical Research Letters, v. 40, p. 2579–2584, doi:10.1002/grl.50375.

Sinha, M., Constable, S., Peirce, C., White, A., Heinson, G., MacGregor, L., and Navin, D., 1998, Magmatic processes at slow spreading ridges: Implications of the RAMESSES experiment at 57°45′ N on the Mid-Atlantic Ridge: Geophysical Journal International, v. 135, p. 731–745, doi:10.1046/j.1365-246X.1998.00704.x.

Sinton, J., and Detrick, R., 1992, Mid-ocean ridge magma chambers: Journal of Geophysical Research, v. 97, p. 197–216, doi:10.1029/91JB02508.

Syracuse, E.M., Thurber, C.H., Wolfe, C.J., Okubo, P.G., Foster, J.H., and Brooks, B.A., 2010, High-resolution locations of triggered earthquakes and tomographic imaging of Kilauea Volcano's south flank: Journal of Geophysical Research, v. 115, B10310, doi:10.1029/2010JB007554.

Thurber, C., 1984, Seismic detection of the summit magma complex of Kilauea volcano, Hawaii: Science, v. 223, p. 165–167, doi:10.1126/science.223.4632.165.

Thurber, C., and Eberhart-Phillips, D., 1999, Local earthquake tomography with flexible gridding: Computers & Geosciences, v. 25, p. 809–818, doi:10.1016/S0098-3004(99)00007-2.

Winterer, E., 1989, Sediment thickness map of the Northeast Pacific, *in* Winterer, E.L., et al., eds., The eastern Pacific Ocean and Hawaii: Boulder, Colorado, Geological Society of America, Geology of North America, v. N, p. 307–310.

Wolfe, C.J., Brooks, B.A., Foster, J.H., and Okubo, P.G., 2007, Microearthquake streaks and seismicity triggered by slow earthquakes on the mobile south flank of Kilauea Volcano, Hawaii: Geophysical Research Letters, v. 34, doi:10.1029/2007GL031625.

Wright, T., and Helz, R., 1996, Differentiation and magma mixing on Kilauea's east rift zone: A further look at the eruptions of 1955 and 1960. Part 2: The 1960 lavas: Bulletin of Volcanology, v. 57, p. 602–630, doi:10.1007/s004450050115.

Wright, T., and Klein, F., 2006, Deep magma transport at Kilauea volcano, Hawaii: Lithos, v. 87, p. 50–79, doi:10.1016/j.lithos.2005.05.004.

Manuscript received 4 August 2013
Revised manuscript received 7 November 2013
Manuscript accepted 11 Novebmer 2013

Printed in USA